BREAST MICROCALCIFICATIONS ENHANCEMENT COMBINING MEAN AND WAVELET FILTERS WITH HISTOGRAM EQUALIZATION

P. C. Carneiro*, A. C. Patrocinio* e A. O. Andrade*

*Laboratory of Biomedical Engineering, Faculty of Electrical Engineering, Federal University of Uberlândia, Uberlândia - MG, Brasil
e-mail: pedrocarneiro@ufu.br

Abstract: Breast cancer is a public health problem that affects countries around the world. Breasts with fibroglandular tissue predominance in their composition are those considered dense breasts. Because fibroglandular tissue and malignant tissue have similar optical densities, visualization of breast cancer may be difficult in breasts of this type (dense). Digital image processing appears as a tool in an attempt to improve the quality of the images, aiding early detection and reducing the intrinsic noise. Thus, the goal of this work is to evaluate the Recursive Mean-separate Histogram Equalization (RMSHE) technique in dense mammographic images containing microcalcifications, after being denoised by arithmetic mean and wavelet filters. The quantitative results indicated that the calculated average SNR values were higher with the enhancement technique. Visually, it was possible to note the effect of denoising through the applied filters in the entire image, and also the microcalcifications contrast enhancement in the regions of interest (ROIs) using the RMSHE technique. From this work it was possible to evaluate the combination of digital filters with recursive technique of histogram equalization, contributing to contrast improvement and structures visualization in dense mammographic images.
Keywords: contrast enhancement, dense breasts, RMSHE, wavelet.

Introduction

The early diagnosis of breast cancer directly influences the mortality rate, and mainly, the possibility of cure of such disease. For this, mammography is the main exam for screening and early detection of breast cancer, being essential for women's health quality [1].

Breast density corresponds to the amount of fatty and fibroglandular tissue present in the breast. This characteristic directly influences the quality of the radiological image, and thus, in the radiologist assessment [2-3].

Some studies [4-6] have related the risk of developing breast cancer with breast density. This means that the higher the breast density, i.e., the greater the predominance of fibroglandular tissue and consequently the greater the risk of breast cancer. One of the reasons for this occurs is the optical density similarity between fibroglandular tissue and the lesion, making difficult the visualization and image assessment.

The digital processing and quality of mammographic images are commonly investigated in order to facilitate the image visualization, aiding in the early diagnosis. Some researches [7-10] have been using both noise filtering and contrast enhancement techniques in order to improve the visualization and characterization of breast structures, such as: nodules, but also microcalcifications.

Therefore, the goal of this work is to evaluate the combination of digital filters (arithmetic mean and wavelet) with a recursive histogram equalization technique in dense mammographic images containing microcalcifications. By calculating the signal-to-noise ratio (SNR) and peak signal-to-noise ratio (PSNR), the idea is to compare the processed images, besides the visual evaluation of regions of interest (ROIs) containing microcalcifications.

Materials and methods

For this work, we used the mammographic images available in the INbreast database, provided by São João Hospital Center in Porto, Portugal [11]. All the database images are fully anonymized, previously assessed by expert staff, saved in Digital Imaging and Communications in Medicine (DICOM) format, and acquired using the same Full-Field Digital Mammography (FFDM) equipment.

By the fact that we have the images assessment, we used in this work, all the images belonging to the class 'd' of breast density (dense breasts) which necessarily contained microcalcifications, totalizing 18 images. The images sizes varies between 3328 x 4084 or 2560 x 3328 pixels, depending on the compression applied in the breast.

The first step of the work was the digital filtering (denoising) in the original images using arithmetic mean and wavelet filters. Equation 1 presents the mean filter function used, where S_{xy} represents the set of coordinates in a rectangular subimage window size of [m,n], centered at point (x,y):

$$\hat{f}(x,y) = \frac{1}{mn}\sum_{(s,t)\in S_{xy}} g(s,t) \quad (1)$$

The arithmetic mean filter [12] computes the average of the neighborhood in the image, reducing the Gaussian noise. In this work, we used window size equal to 3x3, since larger window sizes increase the image blur.

After the mean filter, we also performed the denoising using discrete wavelet transform in the 18 images. Féjer-Korovkin [13] with four taps and one level of decomposition was selected after experimental tests. The threshold calculation was based on Kovesi [14], being applied to the detail coefficients. Finally, the inverse wavelet transform is applied using the approximation, combined with the vertical, horizontal and diagonal coefficients after the thresholding.

For the contrast enhancement the Recursive Mean-separate Histogram Equalization (RMSHE) was used. In the algorithm proposed by Chen and Ramli, in 2003 [15], the image is separated in two subimages based in the pixel average calculation of the original image. After the separation, the two subimages histograms are equalized, and the separation using the average calculation is done recursively. The larger the average separation, the brighter the original image is preserved in contrast enhancement. We used the maximum number of recursions possible for each processed (mean + wavelet denoising) image.

The quantitative analysis was done by calculating the signal-to-noise ratio (SNR) and peak signal-to-noise ratio (PSNR). The SNR can be calculated according to Equation 2, where A_{Signal} and A_{Noise} are the magnitude of the signal and the noise, respectively.

$$\mathrm{SNR_{db}} = 10\log_{10}\left[\left(\frac{\mathrm{Asignal}}{\mathrm{Anoise}}\right)^2\right] \quad (2)$$

The noise is considered as the difference between the resulting (processed images) and the original images. This is the reason why it was not possible to calculate the SNR value of the original image, for comparison purposes. A high SNR value suggest that the noise effect is less than the signal measurement effect [16].

The PSNR is defined by the relation between the signal maximum energy (power) and the noise power [16]. Equation 3 presents the PSNR calculation, where L is equal to 4096 (images number of bits) and MSE is the mean squared error.

$$\mathrm{PSNR_{db}} = 10\log_{10}\left(\frac{(L-1)^2}{MSE}\right) \quad (3)$$

In summary, we obtained two sets of images: one containing the 18 images processed with mean and wavelet filters (mean + wavelet) and the other containing the previous 18 images with the digital filters combined with the RMSHE contrast enhancement technique (mean + wavelet + RMSHE). The average and standard deviation of SNR and PSNR were calculated for these two sets of images. In addition, we selected some regions of interest (ROIs) containing microcalcifications for a visual analysis.

Results

Table 1 presents the calculated SNR and PSNR values for the resulting 18 images of each processing: denoising and contrast enhancement. The average and standard deviation were calculated facilitating the data interpretation and comparison.

Table 1: Average and standard deviation of the calculated SNR and PSNR values for the 18 processed images.

Images	SNR ($X \pm \sigma$)	PSNR ($X \pm \sigma$)
1) Mean + Wavelet	21.93 ± 1.18	71.88 ± 1.38
2) Mean + Wavelet + RMSHE	23.13 ± 1.2	70.08 ± 1.21

In addition to the quantitative analysis, a visual evaluation of the images was also done. Figure 1 and Figure 2 shows different examples of original images (Figure 1A and 2A), and the two resulting images after the processing: denoising (Figure 1B and 2B) and contrast enhancement (Figure 1C and 2C). Further, there are shown the respective cropped regions of interest (ROI) containing microcalcifications.

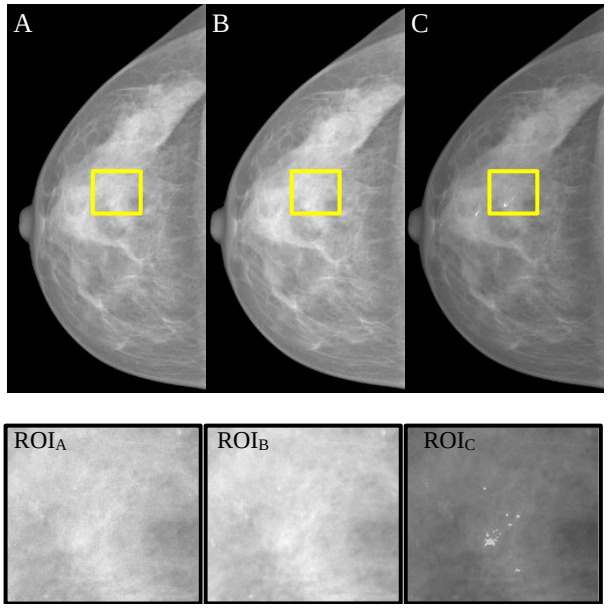

Figure 1: Images and the respective ROIs demarcated in yellow. (A) Original image without processing. (B) Original image denoised with mean and wavelet. (C) Denoised image (mean + wavelet) combined with RMSHE contrast enhancement technique.

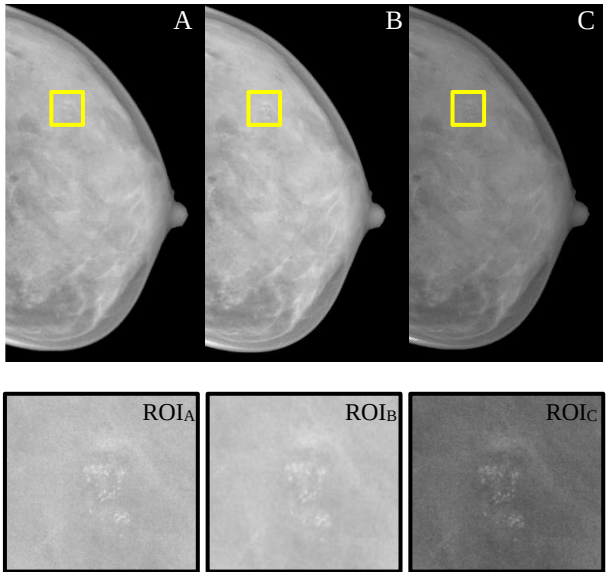

Figure 2: Images and the respective ROIs demarcated in yellow. (A) Original image without processing. (B) Original image denoised with mean and wavelet. (C) Denoised image (mean + wavelet) combined with RMSHE contrast enhancement technique.

Discussion

Analyzing Table 1, the results of both SNR and PSNR were similar, but it is observed that the highest average value of SNR was obtained by combining the denoised methods (mean and wavelet) with the recursive histogram equalization technique. This can be explained since there was noise reduction by the filters, and the RMSHE algorithm was able to promote an increase in the signal, compared to the noise.

However, this fact did not occur in the PSNR calculation. Although the PSNR values for the two image processing were similar (71.88 and 70.08, respectively), the contrast enhancement applied did not promote an increase in the peak signal in relation to the noise.

From Figure 1 and Figure 2 it is possible to visually verify the effect of the applied techniques in the image. By Figure 1(B) and Figure 2(B), despite the similarity with the original one (Figure 1A and 2A), it was noted the noise reduction, since the structures were better defined and identified, mainly by wavelet denoising [10].

In the meantime, in the ROI_B of both figures, we verified that the arithmetic mean filter caused a small blur effect in the image, justifying the small window size (3x3) applied, since larger windows would increase this blurring effect.

On the other hand, the RMSHE application (Figures 1C, 2C, and the respective ROIs) allowed the midrange pixel tones to be more towards the edges, that is, the lighter pixels became even clearer, and the darker ones became even darker. In addition, the tests showed that the maximum number of recursions used, could promote a greater similarity between original and processed image, in agreement with the literature [15].

Conclusion

Filtering as a stage of image preprocessing is an important aspect in digital processing. Mammographic images have intrinsic noises due to the image acquisition itself, which makes essential the noise filtering. With this work, the use of arithmetic mean and wavelet filter for denoising, avoided that during contrast enhancement process, noisy signal were also enhanced.

It was possible to evaluate the RMSHE contrast enhancement technique in the filtered images, verifying both the quantitative values and the visual evaluation . It is worth to highlight the importance of the visual assessment, since the calculated measurements may not be analyzed isolated, and vice versa.

The RMSHE was able to increase the signal in relation to the noise, besides providing the brightness preservation, obtaining satisfactory results for the regions of interest containing microcalcifications.

The next steps of the work are the implementation of new digital filtering and contrast enhancement techniques, especially in dense breasts, providing new tools to aid in the early diagnosis of breast cancer.

Acknowledgements

The authors are thankful for the financial support of CAPES and for Breast Research Group, INESC Porto, Portugal, for making available the image database.

References

[1] Azevedo RL, Gerótica RMG, Sanches TP. A importância da mamografia no diagnóstico precoce do câncer de mama. UNILUS Ensino e Pesquisa. 2016; 13(30):251.

[2] Varghese JS, Thompson DJ, Michailidou K, Lindström S, Turnbull C, Brown, J, Wareham NJ. Mammographic breast density and breast cancer: evidence of a shared genetic basis. Cancer Research. 2012; 3295.

[3] Sickles EA, D'Orsi CJ, Bassett LW, Appleton CM, Berg WA, Burnside E. ACR BI-RADS® Mammography. ACR BI-RADS® Atlas, Breast Imaging Reporting and Data System. Reston, VA, American College of Radiology; 2013.

[4] Pinsky RW, Helvie MA. Mammographic breast density: effect on imaging and breast cancer risk. Journal of the National Comprehensive Cancer Network. 2010; 8(10):1157-1165.

[5] Vachon CM, Van Gils CH, Sellers TA, Ghosh K, Pruthi S, Brandt KR, Pankratz VS. Mammographic density, breast cancer risk and risk prediction. Breast Cancer Research. 2007; 9(6):217.

[6] McCormack VA, Silva IS. Breast density and parenchymal patterns as markers of breast cancer risk: a meta-analysis. Cancer Epidemiology Biomarkers & Prevention. 2006; 15(6): 1159-1169.

[7] Dippel S, Stahl M, Wiemker R, Blaffert T. Multiscale contrast enhancement for radiographies: Laplacian pyramid versus fast wavelet transform. IEEE Transactions on Medical Imaging. 2002; 21(4):343-353.

[8] Nababan EB, Iqbal M, Rahmat RF. Breast cancer identification on digital mammogram using Evolving Connectionist Systems. In: Informatics and Computing (ICIC), International Conference on. IEEE; 2016 Oct 28-29; Lombok, Indonesia. 2016. p. 132-136.

[9] AbuBaker AA. Automatic microcalcification detection using wavelet transform. International Journal of Computer Theory and Engineering. 2015; 7(1):40.

[10] Dong M, Guo YN, Ma YD, Ma YR, Lu XY, Wang KJ. A new study on mammographic image denoising using multiresolution techniques. In: Eighth International Conference on Machine Vision (ICMV 2015); 2015 Dec. 2015(9875). p. 987518.

[11] Moreira IC, Amaral I, Domingues I, Cardoso A, Cardoso MJ, Cardoso JS. INbreast: toward a full-field digital mammographic database. Academic radiology. 2012; 19(2): 236-248

[12] Gonzalez RC, Woods RE. Digital Image Processing. Upper Saddle River, NJ: Prentice Hall, 2007.

[13] Nielsen M. On the construction and frequency localization of finite orthogonal quadrature filters. Journal of Approximation Theory. 2001;108(1): 36-52.

[14] Kovesi P. Phase preserving denoising of images. Signal. 1999; 4(1).

[15] Chen SD, Ramli AR. Contrast enhancement using recursive mean-separate histogram equalization for scalable brightness preservation. IEEE Transactions on Consumer Electronics. 2003;49(4):1301-1309.

[16] Bushberg JT, Boone JM. The essential physics of medical imaging. Lippincott Williams & Wilkins, 2011.